Atmos. Chem. Phys. Discuss., doi:10.5194/acp-2017-434, 2017
Manuscript under review for journal Atmos. Chem. Phys.
Discussion started: 19 May 2017
© Author(s) 2017. CC-BY 3.0 License.

Atmospheric Chemistry and Physics Discussions

Impacts of Stratospheric Sulfate Geoengineering on Tropospheric Ozone

Lili Xia[1*], Peer J. Nowack[2], Simone Tilmes[3], and Alan Robock[1]

[1]Department of Environmental Sciences, Rutgers University, New Brunswick, New Jersey, USA

[2]Centre for Atmospheric Science, Department of Chemistry, University of Cambridge, Cambridge, UK

[3]Atmospheric Chemistry Division, National Center of Atmospheric Research, Boulder, CO, USA

*To whom correspondence should be addressed: Lili Xia, Department of Environmental Sciences, Rutgers University, 14 College Farm Road, New Brunswick, NJ 08901-8551. E-mail: lxia@envsci.rutgers.edu.

Atmos. Chem. Phys. Discuss., doi:10.5194/acp-2017-434, 2017
Manuscript under review for journal Atmos. Chem. Phys.
Discussion started: 19 May 2017
© Author(s) 2017. CC-BY 3.0 License.

Atmospheric Chemistry and Physics Discussions

Abstract

A range of solar radiation management (SRM) techniques has been proposed to counter anthropogenic climate change. Here, we examine the potential effects of stratospheric sulfate aerosol and solar insolation reduction on tropospheric ozone and ozone at Earth's surface. Ozone is a key air pollutant, which can produce respiratory diseases and crop damage. Using a version of the Community Earth System Model from the National Center for Atmospheric Research that includes comprehensive tropospheric and stratospheric chemistry, we model both stratospheric sulfur injection and solar irradiance reduction schemes, with the aim of achieving equal levels of surface cooling relative to the Representative Concentration Pathway 6.0 scenario. This allows us to compare the impacts of sulfate aerosol and solar dimming on atmospheric ozone concentrations. Despite nearly identical global mean surface temperatures for the two SRM approaches, solar insolation reduction increases global average surface ozone concentrations while sulfate injection decreases it. A key difference between the two geoengineering schemes is the importance of heterogeneous reactions in the photochemical ozone balance with larger stratospheric sulfate abundance, resulting in increased ozone depletion in mid- and high latitudes. This reduces the net transport of stratospheric ozone into the troposphere and thus is a key driver of the overall decrease in surface ozone. At the same time, the change in stratospheric ozone alters the tropospheric photochemical environment due to enhanced ultraviolet radiation. A shared factor among both SRM scenarios is decreased chemical ozone loss due to reduced tropospheric humidity. Under insolation reduction, this is the dominant factor giving rise to the global surface ozone increase. Regionally, both surface ozone increases and decreases are found for both scenarios, that is, SRM would affect regions of the world differently in terms of air pollution. In conclusion, surface ozone and tropospheric chemistry would likely be affected by SRM, but the overall effect is strongly dependent on the

Atmos. Chem. Phys. Discuss., doi:10.5194/acp-2017-434, 2017
Manuscript under review for journal Atmos. Chem. Phys.
Discussion started: 19 May 2017
© Author(s) 2017. CC-BY 3.0 License.

Atmospheric Chemistry and Physics Discussions

SRM scheme. Due to the health and economic impacts of surface ozone, all these impacts should be taken into account in evaluations of possible consequences of SRM.

Atmos. Chem. Phys. Discuss., doi:10.5194/acp-2017-434, 2017
Manuscript under review for journal Atmos. Chem. Phys.
Discussion started: 19 May 2017
© Author(s) 2017. CC-BY 3.0 License.

Atmospheric Chemistry and Physics Discussions

1 Introduction

1.1 Atmospheric Ozone

It is well known that sulfate aerosols in the stratosphere enhance heterogeneous chemical reactions that lead to ozone depletion. With present day anthropogenic halogen loading, the aerosols provide surface area for heterogeneous reactions that activate halogens and hence increase catalytic ozone destruction, especially in high latitudes (Tie and Brasseur, 1995). This has been modeled and observed following the large 1982 El Chichón and 1991 Pinatubo volcanic eruptions (Tie and Brasseur, 1995; Portman et al., 1996; Solomon, 1999).

However, volcanic eruptions do not only affect stratospheric ozone, but also impact tropospheric composition, often due to stratosphere-troposphere coupled effects. The 1991 Pinatubo eruption, for example, has been linked to changes in stratosphere-troposphere exchange (STE) of ozone (Aquila et al., 2012; Aquila et al., 2013; Pitari et al., 2016). In addition, the stratospheric ozone decrease led to an invigorated photochemical environment in the troposphere due to enhanced downward chemically-active ultraviolet (UV) radiation (Tang et al., 2013).

This study focuses on tropospheric ozone, in particular surface ozone concentration changes. Surface ozone is of central importance to Earth's environment and as an air pollutant it adversely impacts human health (e.g., Kampa and Castanas, 2008) and the ecosystem (e.g., Mauzeral and Wang, 2001; Ashmore, 2005; Ainsworth et al., 2012). There have been numerous studies of the observed surface ozone trend (e.g., Cooper et al., 2014), identifying ozone sources and sinks (e.g., Wild, 2007), predicting future changes (e.g., Young et al., 2013), and understanding the impacts of such changes (e.g., Silva et al., 2013). Global surface ozone concentrations are estimated to have doubled since the preindustrial period (Vingarzan, 2004), mainly due to increased emissions of ozone precursors associated with industrialization (e.g.,

Atmos. Chem. Phys. Discuss., doi:10.5194/acp-2017-434, 2017
Manuscript under review for journal Atmos. Chem. Phys.
Discussion started: 19 May 2017
© Author(s) 2017. CC-BY 3.0 License.

Atmospheric Chemistry and Physics Discussions

Forster et al., 2007). Differences in future tropospheric ozone concentrations will be strongly dependent on the emission pathway followed (Stevenson et al., 2006), which will determine both in-situ tropospheric chemical production of ozone and transport from the ozone-rich stratosphere (Collins et al., 2003; Wild et al., 2012; Neu et al., 2014).

1.2 Differences between sulfate and solar geoengineering

The progression of global warming, slow mitigation efforts, and our relatively limited adaptive capacity, force consideration of SRM geoengineering as one possible strategy to avoid many of the most undesirable consequences of global warming (Crutzen, 2006; Wigley, 2006; Tilmes, 2016a). The above discussed factors controlling tropospheric ozone concentrations could be affected by SRM schemes (Nowack et al., 2016). Here we compare a proposed geoengineering scheme, stratospheric sulfur injection, to solar irradiance reduction. Both schemes would cool Earth's surface by reducing sunlight reaching the surface, either by aerosols reflecting sunlight or by artificially reducing the solar constant in a climate model, but sulfate geoengineering would strongly heat the stratosphere and provide aerosol surfaces for chemical reactions. Previous studies have shown that injected sulfur chemically forms sulfate aerosols within a couple of weeks. The aerosol layer absorbs near infrared solar radiation as well as outgoing longwave radiation and results in stratospheric warming (e.g., Tilmes et al., 2009; Ammann et al., 2010; Jones et al., 2011). Additionally changes in ozone and advection impact the warming in the stratosphere (Richter et al., 2017, submitted). Under solar reduction, the stratosphere would be cooler due to reduced shortwave heating (Govindasamy and Caldeira, 2000), although simultaneous stratospheric ozone changes (if considered) may buffer this effect (Nowack et al., 2016).

Atmos. Chem. Phys. Discuss., doi:10.5194/acp-2017-434, 2017
Manuscript under review for journal Atmos. Chem. Phys.
Discussion started: 19 May 2017
© Author(s) 2017. CC-BY 3.0 License.

Atmospheric Chemistry and Physics Discussions

96 One of the most important differences between the two scenarios is that if a permanently
97 enhanced stratospheric aerosol layer is artificially created in an attempt to reduce anthropogenic
98 global warming, the resulting strong ozone depletion, in particular in mid- and high latitudes,
99 would have serious impacts on the biosphere, similar to the effects observed after large volcanic
100 eruptions described above (Crutzen, 2006; Rasch et al., 2008a; Rasch et al., 2008b; Tilmes et al.,
101 2008, 2009, 2012). This effect would have to be expected as long as there is anthropogenic
102 halogen in the stratosphere. In the remote future, the decreasing burden of anthropogenic
103 halogen components will eventually result in an increase in stratospheric ozone due to the
104 importance of heterogeneous reactions to the nitrogen cycle in the upper stratosphere, which
105 increases ozone in the middle and upper stratosphere (Tie and Brasseur, 1995; Pitari et al, 2014).
106 Overall such changes to the stratosphere would also have important implications for tropospheric
107 composition. Decreasing stratospheric ozone leads to more UV propagating through, with
108 increasing ozone having the opposite effect, which would thus alter the photochemical
109 environment of the troposphere in different ways (Tilmes et al., 2012; Nowack et al., 2016).

110 In the following sections, we describe the experimental set-up of the two geoengineering
111 schemes and discuss some general climate impacts, followed by a detailed discussion of
112 tropospheric and surface ozone changes. We also show that sulfate and solar geoengineering
113 would impact the stratosphere differently, which implies further key differences in their potential
114 influences on tropospheric composition. In this study, we examine the impacts of stratospheric
115 sulfate geoengineering on tropospheric ozone for the first time.

116 **2 Model and Experiment Design**

117 We simulated both types of SRM schemes using the full tropospheric and stratospheric
118 chemistry version of the Community Earth System Model – Community Atmospheric Model 4

Atmos. Chem. Phys. Discuss., doi:10.5194/acp-2017-434, 2017
Manuscript under review for journal Atmos. Chem. Phys.
Discussion started: 19 May 2017
© Author(s) 2017. CC-BY 3.0 License.

(CESM CAM4-chem) with horizontal resolution of 0.9° x 1.25° lat-lon and 26 levels from the surface to about 40 km (3.5 mb). The model has been shown to give a good representation of present-day atmospheric composition in the troposphere (Tilmes et al., 2016b) and stratosphere at 2° resolution (Fernandez et al., 2017). Similar to the 2° model version, the 1° horizontal resolution version of the model also produces reasonable stratosphere and troposphere ozone chemistry (Figs. S1-S2). CAM4-chem is fully coupled to the Community Land Model version 4.0 with prescribed satellite phenology (CLM4SP), the Parallel Ocean Program version 2 (POP2) ocean model and the Los Alamos sea ice model (CICE version 4). The model uses a nudged quasi-biennial oscillation (QBO), which means the QBO will not be modified by the radiative interaction of the aerosol. Interaction between aerosol burden and photolysis rates is not included in the model. Changes in photolysis rates in the troposphere are calculated depending on the total ozone column change (Kinnison et al., 2007). Volatile organic compound (VOC) emissions are simulated by the Model of Emission of Gases and Aerosols from Nature (MEGAN v2.1) (Guenther et al., 2012). The dynamical ocean model does not include any biogeochemical feedbacks and only the atmospheric and land models are coupled to the atmospheric chemistry component. The model configuration used here, at 2° resolution, is participating in the current phase of the Chemistry-Climate Model Initiative (Tilmes et al., 2016b).

We compare three ensemble members each of the two geoengineering scenarios to a three-ensemble reference run with Representative Concentration Pathway 6.0 (RCP6.0; Meinshausen et al., 2011) anthropogenic forcing from 2020 to 2089. Our sulfate aerosol implementation is the G4 Specified Stratospheric Aerosol (G4SSA) experiment (Tilmes et al., 2015), whereas solar reduction geoengineering is the solar analog (hereafter G4SSA-S) by imposing a solar irradiance reduction with the same negative radiative forcing at the top of the

Atmos. Chem. Phys. Discuss., doi:10.5194/acp-2017-434, 2017
Manuscript under review for journal Atmos. Chem. Phys.
Discussion started: 19 May 2017
© Author(s) 2017. CC-BY 3.0 License.

Atmospheric Chemistry and Physics Discussions

atmosphere (TOA) as in G4SSA. G4SSA uses a prescribed stratospheric aerosol surface area distribution to mimic the effects of continuous emission into the tropical stratosphere at 60 mb of 8 Tg SO_2 yr^{-1} from 2020 to 2069. More details of this prescribed stratospheric aerosol are given in Tilmes et al. (2015b) and Xia et al. (2016). The G4SSA scenario then continues from 2070 to 2089 without imposed aerosols to study the termination effect of geoengineering. During the sulfate injection period, the net solar flux at the TOA has been decreased by 2.5 W/m^2 compared to RCP6.0 (Fig. 1a). This number was obtained by a double radiation call in the model in calculating the direct forcing of the prescribed aerosol layer. To attain the same TOA solar flux reduction in G4SSA-S, we reduced the total solar insolation by 14.7 W/m^2 during 2020-2069 assuming a global average planetary albedo of 0.32 ($14.7\ W/m^2 = \frac{2.5\ W/m^2 \times 4}{1.0 - 0.32}$) (Fig. 1b). From 2070 on, we accordingly reset the total solar insolation back to the reference level to simulate the abrupt termination of geoengineering.

3 Results and Discussion

3.1 Climatology in G4SSA and G4SSA-S

As a consequence of the same net all-sky TOA solar flux reduction in G4SSA and G4SSA-S (Fig. 1a), the two scenarios show approximately the same global mean surface temperature reduction of 0.8 K compared with RCP6.0 (Fig. 2a) (all values below are the average of years 2030-2069). After the termination of geoengineering on 1 January 2070, the global mean surface temperature rapidly increases. Fig. 3 shows the surface temperature differences between G4SSA, G4SSA-S, and RCP6.0 in years 2030-2069 (the last 40 years of geoengineering). Consistent with the global average temperature change, the two geoengineering scenarios have similar temperature reduction patterns (Fig. 3a and 3b), and the differences between them are not significant in most regions (Fig. 3c). The warming in northern

Atmos. Chem. Phys. Discuss., doi:10.5194/acp-2017-434, 2017
Manuscript under review for journal Atmos. Chem. Phys.
Discussion started: 19 May 2017
© Author(s) 2017. CC-BY 3.0 License.

Europe and Asia shown in Fig. 3c is stronger in Northern Hemisphere winter (Fig. S3), which is the characteristic "winter warming" from volcanic stratospheric aerosol (Robock, 2000). However, the zonal mean stratospheric temperatures in G4SSA and G4SSA-S differ substantially (Fig. 4). As shown in previous studies (Tilmes et al., 2009; Ammann et al., 2010; Jones et al., 2011), sulfate aerosol in the stratosphere results in strong warming by 3 K in the tropics (Fig. 4a), while in G4SSA-S there is slight cooling (Fig. 4b). In both cases, the troposphere shows strong temperature reduction with similar patterns and ranges.

Global averaged precipitation and evaporation have similar size reductions of 0.07 mm/day in the two scenarios (Fig. 2c and Fig. S4), with no statistically significant difference between them. Most of the evaporation terms show a larger reduction in G4SSA than in G4SSA-S, except for plant transpiration, which has the opposite pattern (Fig. S4). As shown by Xia et al. (2016), enhanced diffuse radiation in G4SSA increases photosynthesis, which produces stronger transpiration. Therefore, transpiration in G4SSA reduces less than in G4SSA-S.

The similar evaporation reduction in G4SSA and G4SSA-S can also be explained by the surface energy budget (Fig. 5). Although we keep the net shortwave radiation at the TOA the same in the two schemes (Fig. 1a), surface net solar radiation reduces more in G4SSA than in G4SSA-S (Fig. 2b and Fig. 5) due to the absorption by sulfate aerosol in the near-infrared. This stronger surface solar forcing in G4SSA-S is mainly balanced by larger net longwave radiation to the atmosphere (Fig. 5). As a result, latent heat changes in the two scenarios are similar.

The precipitation and evaporation changes in this study are different from previous studies by Niemeier et al. (2013) and Ferraro et al. (2014). In their studies, with the same magnitude of surface cooling, the sulfate injection scenario led to a greater reduction of globally averaged evaporation and precipitation as compared with the solar case. They attribute this

Atmos. Chem. Phys. Discuss., doi:10.5194/acp-2017-434, 2017
Manuscript under review for journal Atmos. Chem. Phys.
Discussion started: 19 May 2017
© Author(s) 2017. CC-BY 3.0 License.

result to extra downwelling longwave radiation because of stratospheric heating from the injected aerosol, which would heat the upper troposphere and stabilize the troposphere compared with the solar reduction case (which we did not find, Fig. 4c), and result in a stronger reduction of latent heat and precipitation in sulfate injection geoengineering. We find two possible reasons for the differences: (1) The column ozone change plays an important role. In Niemeier et al. (2013) and Ferraro et al. (2014), the same prescribed ozone was used in all scenarios, while we used a fully coupled atmosphere-chemistry model. As shown in section 3.2, total column ozone in G4SSA reduces by about 5 DU (mainly in the lower stratosphere) compared with RCP6.0 and G4SSA-S (Fig. 6). Less ozone in G4SSA will change its radiative forcing, surface radiative fluxes and atmospheric lapse rate (Chiodo and Polvani, 2015; MacIntosh et al., 2016; Nowack et al., 2015, 2017) and thus contribute to the differences between the two studies. (2) Enhanced transpiration in G4SSA due to enhanced diffuse radiation reduces the evaporation difference in the two SRM schemes as discussed above.

3.2 Surface and tropospheric ozone response

The ozone response is remarkably different in G4SSA and G4SSA-S. Global mean surface ozone increases under G4SSA-S and decreases under G4SSA, relative to RCP6.0 (Fig. 6a). The total ozone column is dominated by stratospheric column ozone, and shows strong reduction under G4SSA compared to RCP6.0, while the increase under G4SSA-S is small (Figs. 6b and 6d). The underlying upward trends of total column ozone as well as stratospheric ozone in all three scenarios are in line with the gradually declining stratospheric halogen content over time (Figs. 6b and 6d). As there is less halogen in the stratosphere towards the end of the geoengineering, stratospheric ozone is recovering (Fig. 6d) and there is less reduction of the total ozone column in G4SSA relative to RCP6.0 (Fig. 6b). The agreement of all curves as concerns

Atmos. Chem. Phys. Discuss., doi:10.5194/acp-2017-434, 2017
Manuscript under review for journal Atmos. Chem. Phys.
Discussion started: 19 May 2017
© Author(s) 2017. CC-BY 3.0 License.

interannual and decadal variations is because of the imposed QBO and 11-year solar cycles in all the runs. The decreasing tropospheric ozone column and surface ozone after year 2060 in all scenarios results from the global ozone precursor emissions decrease following the RCP6.0 scenario (Young et al., 2013).

The surface ozone concentration distributions in the three scenarios are similar, with the highest concentration over the continents in the Northern Hemisphere (NH) (Fig. S5), while the concentration differences between scenarios are spatially variable (Fig. 7). This highlights that the key driver behind the absolute surface ozone abundances is the underlying ozone precursor emissions following the RCP6.0 scenario. SRM is only a modulating factor, but depending on the SRM scheme even the sign of its impact can differ; global mean surface ozone concentrations in G4SSA are lower, relative to RCP6.0, whereas there are mild surface ozone increases over the tropics (Fig. 7a). The strongest surface ozone reductions compared with RCP6.0 occur in NH mid-latitudes across all seasons (Figs. S6a-d) and Southern Hemisphere (SH) mid-to-high latitudes in MAM and JJA (Figs. S6b, c). As discussed in the next section, the reduction over the continents is related to atmospheric chemistry changes while the reduction over the polar regions in the winter hemisphere is due to transport. In G4SSA-S, surface ozone also increases in the tropics relative to RCP6.0 (Fig. 7b), and this regional change is greater than in G4SSA (Fig. 7c). Surface ozone decreases, however, are found at NH mid-latitudes over the continents during all seasons (Fig. S6e-h). Comparing the two types of geoengineering experiments directly, surface ozone concentrations are generally lower in G4SSA than in G4SSA-S (Fig. 7c), with peak differences in terms of absolute changes (ppb) at SH mid-to-high latitudes in MAM and JJA (Fig. S6i, j) and at NH mid-to-high latitudes in DJF (Fig. S6l).

Atmos. Chem. Phys. Discuss., doi:10.5194/acp-2017-434, 2017
Manuscript under review for journal Atmos. Chem. Phys.
Discussion started: 19 May 2017
© Author(s) 2017. CC-BY 3.0 License.

Atmospheric Chemistry and Physics Discussions

3.3 Mechanisms of surface ozone change

Surface ozone concentrations are determined by chemical production and loss controlled by emissions of ozone precursors and the composition of the atmosphere, loss due to surface deposition of ozone, and the transport of ozone from other regions of the atmosphere (Monks et al., 2015). Since all scenarios considered here are based on the same RCP6.0 emission scenario of ozone precursors, such as nitrogen oxide (NO_x) and methane (CH_4), the differences in surface ozone must necessarily be driven by changes in climate in response to the geoengineering interventions, which include changes in temperature, humidity, atmospheric dynamics, and the photochemical environment. To understand the differences mechanistically, it is helpful to consider the impact of geoengineering on the tropospheric ozone budget.

The upper part of Table 1 shows the sources (production and net transport from the stratosphere (stratosphere-troposphere-exchange, STE)) and sinks (loss rates and dry deposition) of tropospheric ozone. Both G4SSA and G4SSA-S show positive net chemical change of tropospheric ozone (chemical production minus loss) and negative change in STE of ozone relative to RCP6.0. However, the magnitude of these changes is significantly different. Compared with RCP6.0, tropospheric ozone net chemical change increases by ~125 Tg yr^{-1} and ~40 Tg yr^{-1} in G4SSA and G4SSA-S, respectively, whereas STE of ozone decreases by ~140 Tg yr^{-1} (~25%) and ~30 Tg yr^{-1} (~5%) in G4SSA and G4SSA-S, respectively. The positive net chemical changes are the result of reductions in both chemical ozone production and loss under G4SSA and G4SSA-S relative to RCP6.0, with larger reductions in ozone loss reactions (Table 1). Specifically, G4SSA-S shows a ~90 Tg yr^{-1} larger decrease in ozone chemical production, whereas ozone loss budgets are reduced by similar magnitudes for the two SRM schemes (262.5 Tg yr^{-1} and 269.5 Tg yr^{-1}). Combining the chemical and transport changes, the tropospheric

Atmos. Chem. Phys. Discuss., doi:10.5194/acp-2017-434, 2017
Manuscript under review for journal Atmos. Chem. Phys.
Discussion started: 19 May 2017
© Author(s) 2017. CC-BY 3.0 License.

Atmospheric Chemistry and Physics Discussions

ozone budget decreases under G4SSA and increases under G4SSA-S relative to RCP6.0, which is consistent with the overall surface ozone changes.

The reasons for these specific changes are discussed in detail in the following two sections. Then, the impacts of the factors are combined to explain regional surface ozone differences, as shown in Fig. 7.

3.3.1 Chemical ozone production and loss in the troposphere

Changes in tropospheric water vapor concentrations and the tropospheric photolysis environment under G4SSA and G4SSA-S are key to understand the differences in tropospheric ozone production and loss. This result is consistent with results of a previous study for the case of solar geoengineering under a more idealized forcing scenario (Nowack et al., 2016).

To explain this, we briefly re-iterate that tropospheric ozone (O_3) production is driven by photolysis of nitrogen dioxide (NO_2) and the subsequent formation of ozone via a three-body-reaction with resulting ground state atomic oxygen $O(^3P)$ (Monks, 2005),

$$NO_2 + h\nu\ (\lambda < 420\ nm) \rightarrow NO + O(^3P) \quad (1)$$

$$O(^3P) + O_2 + M \rightarrow O_3 + M \quad (2)$$

where M is an inert collision partner (mostly molecular nitrogen). NO_2 formation in turn is crucially dependent on the oxidation of NO by reaction with peroxides present in the troposphere, for example,

$$HO_2 + NO \rightarrow NO_2 + OH \quad (3)$$

$$RO_2 + NO \rightarrow NO_2 + RO \quad (4)$$

where R represents general organic residues such as CH_3 (row 6 in Table 1). RO_2 in turn is produced by oxidation reactions between VOCs and the hydroxyl radical OH. Tropospheric OH

Atmos. Chem. Phys. Discuss., doi:10.5194/acp-2017-434, 2017
Manuscript under review for journal Atmos. Chem. Phys.
Discussion started: 19 May 2017
© Author(s) 2017. CC-BY 3.0 License.

Atmospheric Chemistry and Physics Discussions

is formed primarily by ozone photolysis and subsequent reaction of excited atomic oxygen $O(^1D)$ with water vapor,

$$O_3 + h\nu\ (\lambda < 320\ nm) \rightarrow O(^1D) + O_2 \quad (5)$$

$$O(^1D) + H_2O \rightarrow 2\ OH \quad (6)$$

Reaction (6) competes with several other reactions due to the high reactivity of $O(^1D)$. However, most importantly, the majority of $O(^1D)$ is quenched by collision with inert molecules such as molecular nitrogen to ground state atomic oxygen $O(^3P)$, which subsequently undergoes reformation to O_3 via three-body-reaction (2). Therefore, tropospheric ozone production and loss is strongly linked to concentrations of water vapor and the photochemical environment (availability of UV) in the troposphere.

In the case of clean (low NO_x) environments, lower water vapor concentrations (mainly in the tropical region 30°N – 30°S) (Fig. S7) lead to less ozone loss via reactions (5) and (6) and additional reactions with the formed HOx species (r-O(1D)-H_2O, r-OH-O_3, and r-HO_2-O_3 in Table 1). This happens at the expense of more quenching of $O(^1D)$ and subsequent recycling of ozone, thus resulting in ozone increases. In contrast, in polluted (high NO_x) environments, less OH formation under lower atmospheric water vapor concentrations leads to reduced formation of RO_2 and HO_2. Therefore, less NO_2 is produced via reactions (3) and (4), resulting in less catalytic ozone production via reactions (1) and (2) (r-NO-HO_2 and e.g. r-CH_3O_2-NO in Table 1). Consequently, ozone production is reduced in NO_x-polluted environments under lower atmospheric water vapor concentrations.

With these fundamentals in mind, it is possible to understand the sign of the tropospheric ozone loss and production rate changes summarized in Table 1. Under both G4SSA and G4SSA-S, the key objective is to achieve surface temperature decreases. Tropospheric water

Atmos. Chem. Phys. Discuss., doi:10.5194/acp-2017-434, 2017
Manuscript under review for journal Atmos. Chem. Phys.
Discussion started: 19 May 2017
© Author(s) 2017. CC-BY 3.0 License.

Atmospheric Chemistry and Physics Discussions

vapor concentrations (or specific humidity) are strongly coupled to surface temperatures, because relative humidity does not change much with climate change (Soden and Held, 2006; Dessler and Sherwood, 2009), so that the surface cooling simultaneously reduces tropospheric specific humidity by 5-20% depending on region and altitude. The slow-down of the hydrological cycle under SRM will further enhance this tropospheric humidity reduction (Bala et al., 2002; Tilmes et al., 2013; Nowack et al., 2016). As a result, less water vapor in both G4SSA and G4SSA-S reduces ozone chemical loss by ~150 Tg yr^{-1} through reactions (5) and (6). The resulting decrease in HO_x leads to further reductions in ozone loss, i.e., via reaction with OH (~20 Tg yr^{-1}) and HO_2 (~60-70 Tg yr^{-1}). Overall, these water vapor/HO_x-related reactions explain ~90% of the overall reduction in ozone loss under SRM compared to a future RCP6.0 simulation.

The reduction in atmospheric humidity also affects ozone production, but to a smaller degree. Here, ozone production via reaction between NO and HO_2 is the key factor in driving these changes, with reductions of ~55 and 120 Tg yr^{-1} for G4SSA and G4SSA-S, respectively. The signal of reduced OH production propagates through all other NO_x-catalyzed ozone production pathways involving RO_2 via reactions (4) and subsequently (1) and (2). NO oxidation via the CH_3O_2-NO pathway decreases by ~27 and 49 Tg yr^{-1} in G4SSA and G4SSA-S. Changes in natural NO_x emissions by lightning play a minor role in comparison. In both SRM schemes, the reduction of lightning induced NO_x is not significant in most regions, and there is no significant difference between the two SRM schemes (Fig. S8).

The changes in chemical ozone production rates tend to be smaller in the sulfate G4SSA experiment than in the case of a solar constant reduction in G4SSA-S. There are three possible factors that contribute to this:

Atmos. Chem. Phys. Discuss., doi:10.5194/acp-2017-434, 2017
Manuscript under review for journal Atmos. Chem. Phys.
Discussion started: 19 May 2017
© Author(s) 2017. CC-BY 3.0 License.

1. The entire reaction cycle depends on the availability of sunlight to photolyse O_3 and NO_2. Since SRM schemes modulate the intensity of sunlight (here by l%) reaching the troposphere in order to mitigate tropospheric warming, this will necessarily also play a role in all changes to ozone production and loss reactions in our SRM simulations. More importantly, however, the sulfate injection geoengineering alters stratospheric ozone concentrations, which ultimately impacts the photochemical environment of the troposphere by changing radiative fluxes into the troposphere (DeMore et al., 1997; Nowack et al., 2016). For example, a reduced stratospheric column will help to stimulate the tropospheric photochemistry by allowing more radiation relevant reactions (1) and (5) to propagate into the troposphere.

2. Diffuse radiation under G4SSA promotes the photosynthesis rate and increases canopy transpiration (Fig. S4). Therefore, we expect that water vapor concentration over the continents with plants would be slightly higher in G4SSA relative to G4SSA-S (Fig. S9). Those regions with higher water vapor (East Asia, South Asia, North America, South Africa) are consistent with high NO_x regions (Fig. S10). Therefore, the slightly smaller reduction of water vapor under G4SSA in the regions above increases ozone chemical production compared with G4SSA-S, and hence G4SSA shows less reduction of ozone chemical production than that in G4SSA-S.

3. Different biogenic VOC emissions under G4SSA and G4SSA-S, which, due to their central role in forming NO_2, are highly important for ozone production. In both scenarios, lower temperatures reduce the heat stress on the emitting plants and therefore reduces their VOC emissions (Tingey et al., 1980; Sharkey and Yeh, 2001; Lathière et al., 2005; Bornman et al., 2015) (e.g., bio-emitted isoprene, Fig. S11). However, at the same time enhanced diffuse radiation under G4SSA increases biogenic VOC emissions compared with G4SSA-S (Wilton et

Atmos. Chem. Phys. Discuss., doi:10.5194/acp-2017-434, 2017
Manuscript under review for journal Atmos. Chem. Phys.
Discussion started: 19 May 2017
© Author(s) 2017. CC-BY 3.0 License.

Atmospheric Chemistry and Physics Discussions

al., 2011) (Fig. S11i, j, k and l). In Table 1, biogenic VOC-related ozone chemical production is generally very similar between G4SSA with G4SSA-S (e.g., r-ISOPO$_2$-NO, r-MACRO$_2$-NOa, r-MCO$_3$-NO and r-TERPO$_2$-NO), and contributes less than 2% to the overall difference between G4SSA and G4SSA-S.

3.3.2 Changes in stratosphere-troposphere exchange

Stratospheric chemical and dynamical changes can impact tropospheric ozone not only by changing the tropospheric photochemical environment, but also by changing the actual transport of ozone from the stratosphere into the troposphere (Hegglin and Shepherd, 2009; Neu et al., 2014). This can be either caused by changes in ozone concentrations in the stratosphere, or by changes in the rate of exchange of air masses between stratosphere and troposphere (i.e., the strength of the Brewer–Dobson (B-D) circulation).

Fig. 8 shows seasonal latitude-height cross-sections of differences in ozone volume mixing ratios between G4SSA and RCP6.0 as well as G4SSA-S and RCP6.0 for altitudes above the 500 mb pressure level. Under G4SSA, heterogeneous reactions on the aerosol surfaces lead to increased halogen activation and with that an enhancement of ozone depletion in mid to high latitudes (Tilmes et al., 2008, 2009, 2012; Heckendorn et al., 2009). On the other hand, heterogenous reactions reduce the NO_x to NO_y ratio, which results in an increase in ozone mixing ratios, mainly in the middle stratosphere (Tie and Brasseur, 1995) (Fig. 8a). In addition, changes in temperature also change the photochemistry of ozone. Altogether, this results in year-round lower stratospheric ozone loss worldwide that peaks during the return of sunlight at high SH latitudes. In comparison, the solar reduction in G4SSA-S does not enhance stratospheric heterogeneous reactions. The much smaller change (increase) in ozone (Fig. 8b) is driven by the change of homogeneous chemistry due to slight temperature reduction (Fig. 4b)

Atmos. Chem. Phys. Discuss., doi:10.5194/acp-2017-434, 2017
Manuscript under review for journal Atmos. Chem. Phys.
Discussion started: 19 May 2017
© Author(s) 2017. CC-BY 3.0 License.

and the slowing of the B-D circulation under tropospheric cooling (Fig. 9b) (Lin and Fu, 2013; Nowack et al., 2015; Shepherd and McLandress, 2011). The net result is small ozone increases in the tropical lower stratosphere and decreases in both extratropical lower stratospheres (Fig. 8b).

Age of air is used to indicate the strength of the B-D circulation (Fig. 9). Here, it is calculated relative to the zonal mean of 1°N at 158.1 mb (Garcia and Randel, 2008; Waugh, 2002). Older air indicates a slow-down of the B-D circulation. Compared with RCP6.0, both G4SSA and G4SSA-S show older air in the stratosphere indicating a slowdown of the circulation. The cooling effect in two SRM scenarios correlates with a weakening of tropical upwelling. However, in G4SSA, the heating of the tropical stratosphere results in enhanced lifting, which counteracts the weakening of the B-D circulation (Figs. 9a and 9c). Previous studies show controversial results on how the B-D circulation changes due to extra aerosol in the atmosphere. Aquila et al. (2012) modeled stronger tropic upwelling after the eruption of Mt. Pinatubo, and other studies also found enhanced simulated B-D circulation after this volcano eruption (Aquila et al., 2013; Pitari et al., 2016). However, with extra black carbon in the stratosphere, the tropical upwelling weakens due to the simultaneous effect of tropospheric cooling (Shepherd and McLandress, 2011; Mills et al., 2014).

The sum of both effects, stratospheric chemical changes and the impact of B-D circulation change on STE of ozone, is shown in Fig. 10. In G4SSA, ozone transported from the stratosphere to the troposphere is significantly decreased by ~25% relative to RCP6.0. In G4SSA-S the reduction is small. Since the air mass transported from the stratosphere to the troposphere is reduced in both scenarios, and is even more strongly reduced under G4SSA-S (Fig. 9), we find that the enhanced stratospheric ozone depletion in G4SSA is the dominant reason for

Atmos. Chem. Phys. Discuss., doi:10.5194/acp-2017-434, 2017
Manuscript under review for journal Atmos. Chem. Phys.
Discussion started: 19 May 2017
© Author(s) 2017. CC-BY 3.0 License.

Atmospheric Chemistry and Physics Discussions

392 the strong reduction of STE of ozone. This is also supported by a stratospheric ozone tracer from
393 the model, O_3^{Strat}, which is set to ozone mixing ratios in the stratosphere and experiences only
394 chemical loss in the troposphere without chemical production (Fig. S12). . We thus conclude
395 that the significant changes in STE of ozone in G4SSA are mainly driven by enhanced
396 stratospheric ozone depletion catalysed through the aerosols (see also Table 1).

397 **3.3 Balance of the different mechanisms**

398 In summary, there are two main factors that determine the tropospheric ozone responses
399 in our SRM and RCP6.0 simulations: (a) changes in tropospheric ozone chemical production/loss
400 due to water vapor changes and impacts on the photochemical environment of the troposphere as
401 a result of both changes in stratospheric ozone and (to a smaller degree) the actual dimming of
402 sunlight depending on the geoengineering scheme, and (b) changes in stratosphere-troposphere
403 exchange of ozone.

404 These factors can also be used to explain the big picture behind the surface ozone
405 changes shown in Fig. 7. In G4SSA-S the reduced tropospheric humidity leads to stronger
406 reductions of ozone loss than the decreases in ozone production, leading to global increases in
407 surface ozone, but particularly in clean air oceanic environments in the tropics. This net increase
408 in ozone chemical change is not cancelled out by the slight reduction of ozone transport from the
409 stratosphere (Fig. 10). In G4SSA, reduction of ozone transport from the stratosphere is the
410 controlling factor, which overwhelms the increase in net ozone production. The effect is
411 particularly pronounced at mid-to-high latitudes (Fig. S12a), thus giving rise to surface ozone
412 decreases there (Fig. 7). In contrast, the effect of reduced tropospheric humidity is relatively
413 more important in the tropics than in other regions, which results in a local increase in surface
414 ozone under G4SSA. Regionally HO_x-NO_x induced reductions in ozone production (Table 1)

Atmos. Chem. Phys. Discuss., doi:10.5194/acp-2017-434, 2017
Manuscript under review for journal Atmos. Chem. Phys.
Discussion started: 19 May 2017
© Author(s) 2017. CC-BY 3.0 License.

415 can become important to explain surface ozone decreases in NO_x-polluted land areas in the NH
416 for both scenarios (Figs. 7 and S6). Further minor contributions to the differences in surface
417 ozone between G4SSA and G4SSA-S are a consequence of changes in water vapor due to
418 regional canopy transpiration effects and biogenic VOC emissions (e.g., isoprene, Table 1 and
419 Fig. S11).

420 **4. Conclusions**

421 Tropospheric ozone changes are to be expected in a geoengineered climate with
422 consequent impacts on air pollution and crop yields. However, for the scenarios considered here,
423 solar and sulfate geoengineering could have entirely different impacts, even in terms of the sign
424 of the response, a rare discrepancy for a surface signal between these two types of
425 geoengineering. There have been many studies using solar irradiance reductions to illustrate
426 SRM. However, it turns out that different SRM strategies would have different impacts on
427 hydrology, atmospheric dynamics, the terrestrial carbon sink, and as investigated in this paper,
428 tropospheric chemistry. These results also depend on the scenario of future ozone precursor and
429 halogen emissions.

430 We have identified and explained the mechanisms by which stratospheric sulfate
431 geoengineering would change surface ozone concentrations. We find that geoengineering might
432 have the potential to significantly reduce some climate impacts, but it cannot fix the problem of
433 air pollution. To reduce air pollution effectively, changes in surface emissions are key, with
434 changes in climate (including geoengineering) being only a modulating factor (Monks et al.,
435 2015; Stevenson et al., 2013; Young et al., 2013). More importantly, the surface ozone reduction
436 between 2030 and 2070 in G4SSA is primarily the result of decreased STE of ozone following
437 ozone depletion in the stratosphere. The rather mild pollution benefit under the RCP6.0

Atmos. Chem. Phys. Discuss., doi:10.5194/acp-2017-434, 2017
Manuscript under review for journal Atmos. Chem. Phys.
Discussion started: 19 May 2017
© Author(s) 2017. CC-BY 3.0 License.

438 background would thus be bought at the expense of the delay of the stratospheric ozone
439 recovery, which would result in enhanced UV penetration to Earth's surface and with that
440 serious impacts on human health (e.g., skin cancer) and the ecosystem. In the future, potential
441 increases of stratospheric ozone as a result of geoengineering may result in an increase of surface
442 ozone, causing more ozone pollution. However, further analysis on air pollutants other than
443 ozone are needed.

444 As shown by Pitari et al. (2014), impacts on ozone from stratospheric geoengineering can
445 be highly model dependent. We consider the results here to be a GeoMIP testbed experiment,
446 and encourage others to compare our results to those from other climate models to evaluate the
447 robustness of the results presented here.

448

449 **Acknowledgments.** This work is supported by U.S. National Science Foundation (NSF) grants
450 AGS-1157525, GEO-1240507, AGS-1430051, and AGS-1617844. Computer simulations were
451 conducted on the National Center for Atmospheric Research (NCAR) Yellowstone
452 supercomputer. NCAR is funded by the NSF. The CESM project is supported by the NSF and
453 the Office of Science (BER) of the US Department of Energy. Peer Nowack is supported by the
454 European Research Council through the ACCI project, project number 267760. We thank Jean-
455 Francois Lamarque, Daniel Marsh, Andrew Conley, Louisa K. Emmons, Rolando R. Garcia,
456 Anne K. Smith, and Douglas E. Kinnison for the CAM4-Chem development.

457

© Author(s) 2017. CC-BY 3.0 License.

References

Ainsworth, E. A., Yendrek, C. R., Sitch, S., Collins, W. J., and Emberson, L. D.: The effects of tropospheric ozone on net primary productivity and implications for climate change, Annual Review of Plant Biology, 63, 637-661, doi:10.1146/annurev-arplant-042110-103829, 2012.

Ammann, C. M., Washington, W. M., Meehl, G. A., Buja, L., and Teng, H.: Climate engineering through artificial enhancement of natural forcings: Magnitudes and implied consequences, J. Geophys. Res., 115, D22109, doi:10.1029/2009JD012878, 2010.

Ashmore, M. R.: Assessing the future global impacts of ozone on vegetation, Plant, Cell and Environment, 28, 949-964, doi:10.1111/j.1365-3040.2005.01341.x, 2005.

Aquila, V., Oman, L. D., Stolarski, R. S., Colarco, P. R., and Newman, P. A.: Dispersion of the volcanic sulfate cloud from a Mount Pinatubo-like eruption, J. Geophys. Res., 117, D06216, doi:10.1029/2011JD016968, 2012.

Aquila, V., Oman, L. D., Stolarski, R. S., Douglass, A. R., and Newman, P. A.: The response of ozone and nitrogen dioxide to the eruption of Mt. Pinatubo at southern and northern midlatitudes, J. Atmos. Sci., 70, 894-900, doi:10.1175/JAS-D-12-0143.1, 2013.

Bala, G., Thompson, S., Duffy, P. B., Caldeira, K. and Delire, C.: Impact of geoengineering schemes on the terrestrial biosphere, Geophys. Res. Lett., 29(22), 14–18, doi:10.1029/2002GL015911, 2002.

Bornman, J. F., Barnes, P. W., Robinson, S. A., Ballaré, C. L., Flint, S. D., and Caldwell, M. M.: Solar ultraviolet radiation and ozone depletion-driven climate change: effects on terrestrial ecosystems, Photochem. Photobiol. Sci., 14, 88-107, doi:10.1039/C4PP90034K, 2015.

Chiodo, G., and Polvani, L. M.: Reduction of climate sensitivity of solar forcing due to stratospheric ozone feedback, J. Clim., 29, 4651-4663, doi: http://dx.doi.org/10.1175/JCLI-D-15-0721.1, 2015.

Collines, W. J., Derwent, R. G., Garnier, B., Johnson, C. E., and Sanderson, M. G.: Effect of stratosphere-troposphere exchange on the future tropospheric ozone trend, J. Geophys. Res., 108 (D12), 8528, doi:10.1029/2002JD002617, 2003.

Cooper, O. R., et al.: Global distribution and trends of tropospheric ozone: An observation-based review, Elementa: Science of the Anthropocene, 2, 000029, doi:10.12952/jounal.elementa.000029, 2014.

Crutzen, P.: Albedo enhancement by stratospheric sulfur injections: A contribution to resolve a policy dilemma? Climatic Change, 77(3), 211-220, doi:10.1007/s10584-006-9101-y, 2006.

DeMore, W. B., Sander, S. P., Golden, D. M., Hampson, R. F., Kurylo, M. J., Howard, C. J., Ravishankara, A. R., Kolb, C. E., and Molina, M. J.: Chemical Kinetics and Photochemical Data for Use in Stratospheric Modeling, Tech. Report, Pasadena, California., 1997.

Dessler, A. E., and Sherwood, S. C.: A matter of humidity, Science, 323, 1020-1021, doi:10.1126/science.1171264, 2009.

Fernandez, R. P., Kinnison, D. E., Lamarque, J-. F., Tilmes, S., and Saiz-Lopes, A.: Impact of biogenic very short-lived bromine on the Antarctic ozone hole during the 21st century, Atmos.

© Author(s) 2017. CC-BY 3.0 License.

497 Chem. Phys., 17, 1673-1688, doi:10.5194/acp-17-1673-2017, 2017.

498 Ferraro, A. J., Highwood, E. J., and Andrew J Charlton-Perez, A. J.: Weakened tropical
499 circulation and reduced precipitation in response to geoengineering, Env. Res. Lett., 9,
500 014001, doi:10.1088/1748-9326/9/1/014001, 2014.

501 Forster, P. et al.: Changes in Atmospheric Constituents and in Radiative Forcing in: Climate
502 Change 2007: The Physical Science Basis. Contribution of Working Group I to the Fourth
503 Assessment Report of the Intergovernmental Panel on Climate Change, Cambridge
504 University Press, Cambridge, United Kingdom and New York, NY, USA, 2007.

505 Garcia, R. R., and Randel, W. J.: Acceleration of the Brewer-Dobson Circulation due to
506 increases in greenhouse gases, J. Atmos. Sci., 65, 2731-2739, doi:10.1175/2008JAS2712.1,
507 2008.

508 Govindasamy, B., and Calderia, K.: Geoengineering Earth's radiation balance to mitigate CO_2-
509 induced climate change, Geophys. Res. Lett., 27, 2141-2144, doi:10.1029/1999GL006086,
510 2000.

511 Guenther, A. B., X. Jiang, C. L. Heald, T. Sakulyanontvittaya, T. Duhl, L. K. Emmons, and X.
512 Wang, 2012: The Model of Emissions of Gases and Aerosols from Nature version 2.1
513 (MEGAN2.1): an extended and updated framework for modeling biogenic emissions. Geosci.
514 Model Dev., **5**, 1471-1492, doi:10.5194/gmd-5-1471-2012.

515 Heckendorn, P., Weisenstein, D., Fueglistaler, S., Luo, B. P., Rozanov, E., Schraner, M.,
516 Thomason, L. W., and Peter, T.: The impact of geoengineering aerosols on stratospheric
517 temperature and ozone, Environ. Res. Lett., 4, 045108, doi:10.10881/1748-9326/4/4/045108,
518 2009.

519 Hegglin, M. I. and Shepherd, T. G.: Large climate-induced changes in ultraviolet index and
520 stratosphere-to-troposphere ozone flux, Nat. Geosci., 2(10), 687–691, doi:10.1038/ngeo604,
521 2009.

522 Jones, A., Haywood, J., and Boucher, O.: A comparison of the climate impacts of
523 geoengineering by stratospheric SO2 injection and by brightening the marine stratocumulus
524 cloud, Atmos. Sci. Let., 12, 176-183, doi:10.1002/asl.291, 2011.

525 Kampa, M., and Castanas, E.: Human health effects of air pollution, Environmental Pollution,
526 151(2), 362-367, doi:10.1016/j.envpol.2007.06.012, 2008.

527 Kinnison, D. E., et al.: Sensitivity of chemical tracers to meteorological parameters in the
528 MOZART-3 chemical transport model. J. Geophys. Res., 112, D20302,
529 doi:10.1029/2006JD007879, 2017.

530 Lamarque, J.-F., Bond, T. C., Eyring, V., Granier, C., Heil, A., Klimont, Z., Lee, D., Liousse, C.,
531 Mieville, A., Owen, B., Schultz, M. G., Shindell, D., Smith, S. J., Stehfest, E., Van Aardenne,
532 J., Cooper, O. R., Kainuma, M., Mahowald, N., Mc- Connell, J. R., Naik, V., Riahi, K., and
533 van Vuuren, D. P.: Historical (1850–2000) gridded anthropogenic and biomass burning
534 emissions of reactive gases and aerosols: methodology and application, Atmos. Chem. Phys.,
535 10, 7017–7039, doi:10.5194/acp-10-7017-2010, 2010.

© Author(s) 2017. CC-BY 3.0 License.

536 Lamarque, J.-F., Emmons, L. K., Hess, P. G., Kinnison, D. E., Tilmes, S., Vitt, F., Heald, C. L.,
537 Holland, E. A., Lauritzen, P. H., Neu, J., Orlando, J. J., Rasch, P. J., and Tyndall, G. K.:
538 CAM-Chem: Description and evaluation of interactive atmospheric chemistry in the
539 Community Earth System Model, Geosci. Model Dev., 5, 369-411, doi:10.5194/gmd-5-369-
540 2012, 2012.

541 Lathière, J., Hauglustaine, D. A., De Noblet-Ducoudré, N., Krinner, G., and Folberth, G. A.: Past
542 and future changes in biogenic volatile organic compound emissions simulated with a global
543 dynamic vegetation model, Geophys. Res. Lett., 32, L20818, doi:10.1029/2005GL024164,
544 2005.

545 MacIntosh, C. R., Allan, R. P., Baker, L. H., Bellouin, N., Collins, W., Mousavi, Z., and Shine,
546 K. P.: Contrasting fast precipitation responses to tropospheric and stratospheric ozone forcing,
547 Geophys. Res. Lett., 43, 1263-1271, doi:10.1002/2015GL067231, 2016.

548 Mauzerall, D. L., and Wang, X. P.: Protecting agricultural crops from the effects of tropospheric
549 ozone exposure: Reconciling science and standard setting in the United States, Europe, and
550 Asia, Annual Review of Energy and the Environment, 26, 237-268,
551 doi:10.1146/annurev.energy.26.1.237, 2001.

552 Meinshausen, M., et al.: The RCP greenhouse gas concentrations and their extension from 1765
553 to 2300, Climatic Change, 109, 213-241, doi:10.1007/s10584-011-0156-z, 2011.

554 Mills, M., Toon, O.B., Lee-Taylor, J., and Robock, A.: Multi-decadal global cooling and
555 unprecedented ozone loss following a regional nuclear conflict, Earth's Future, 2, 161-176,
556 doi:10.1002/2013EF000205, 2014.

557 Monks, P. S.: Gas-phase radical chemistry in the troposphere., Chem. Soc. Rev., 34(5), 376–395,
558 doi:10.1039/b307982c, 2005.

559 Monks, P. S., Archibald, A. T., Colette, A., Cooper, O., Coyle, M., Derwent, R., Fowler, D.,
560 Granier, C., Law, K. S., Mills, G. E., Stevenson, D. S., Tarasova, O., Thouret, V., Von
561 Schneidemesser, E., Sommariva, R., Wild, O. and Williams, M. L.: Tropospheric ozone and
562 its precursors from the urban to the global scale from air quality to short-lived climate forcer,
563 Atmos. Chem. Phys., 15(15), 8889–8973, doi:10.5194/acp-15-8889-2015, 2015.

564 Neu, J. L., Flury, T., Manney, G. L., Santee, M. L., Livesey, N. J. and Worden, J.: Tropospheric
565 ozone variations governed by changes in stratospheric circulation, Nat. Geosci., 7(5), 340–
566 344, doi:10.1038/NGEO2138, 2014.

567 Niemeier, U., Schmidt, H., Alterskjær, K., and Kristjánsson, J. E.: Solar irradiance reduction via
568 climate engineering: Impact of different techniques on the energy balance and the
569 hydrological cycle, J. Geophys. Res. Atmos., 118, 11,905-11,917,
570 doi:10.1002/2013JD020445, 2013.

571 Nowack, P. J., Abraham, N. L., Maycock, A. C., Braesicke, P., Gregory, J. M., Joshi, M. M.,
572 Osprey, A. and Pyle, J. A.: A large ozone-circulation feedback and its implications for global
573 warming assessments, Nat. Clim. Chang., 5(1), 41–45, doi:10.1038/nclimate2451, 2015.

574 Nowack, P. J., Abraham, N. L., Braesicke, P. and Pyle, J. A.: Stratospheric ozone changes under
575 solar geoengineering: implications for UV exposure and air quality, Atmos. Chem. Phys., 16,
576 4191–4203, doi:10.5194/acpd-15-31973-2015, 2016.

© Author(s) 2017. CC-BY 3.0 License.

577 Nowack, P. J., Braesicke, P., Abraham, N. L., and Pyle, J. A.: On the role of ozone feedback in
578 the ENSO amplitude response under global warming, Geophys. Res. Lett., 44,
579 doi:10.1002/2016GL072418, 2017.

580 Pitari, G., Aquila, V., Kravitz, B., Robock, A., Watanabe, S., Cionni, I., De Luca, N., Genova, G.
581 I., Mancini, E., and Tilmes, S.: Stratospheric ozone response to sulfate geoengineering:
582 Results from the Geoengineering Model Intercomparison Project (GeoMIP). J. Geophys. Res.
583 Atmos., 119, 2629-2653, doi:10.1002/2013JD020566, 2014.

584 Pitari, G., Cionni, I., Genova, G. D., Visioni, D., Gandolfi, I., and Mancini, E.: Impact of
585 stratospheric volcanic aerosols on age-of-air and transport of long lived species, Atmosphere,
586 7 (11), 149, doi:10.3390/atmos7110149, 2016.

587 Portmann, R. W., Solomon, S., Garcia, R. R., Thomason, L. W., Poole, L. R., and McCormick,
588 M. P.: Role of aerosol variations in anthropogenic ozone depletion in the polar regions, J.
589 Geophys. Res., 101, D17, 22,991-23,006, doi:10.1029/96JD02608, 1996.

590 Rasch, P. J., Crutzen, P. J., and Coleman, D. B.: Exploring the geoengineering of climate using
591 stratospheric sulfate aerosols: The role of particle size, J. Geophys. Res., 35, L02809,
592 doi:10.1029/2007GL032179, 2008a.

593 Rasch, P. J., Tilmes, S., Turco, R. P., Robock, A., Oman, L., Chen, C-C., Stenchikov, G. L., and
594 Garcia, R. R.: An overview of geoengineering of climate using stratospheric sulphate
595 aerosols, Phil. Trans. R. Soc. A., 366, 4007-4037, doi:10.1098/rsta.2008.0131, 2008b.

596 Robock, A.: Volcanic eruption and climate, Rev. Geophys., 38, 191-219,
597 doi:10.1029/1998RG000054, 2000.

598 Sharkey, T. D., and Yeh, S. S.: Isoprene emission from plants. Ann. Rev. Plant Phys. Plant Mol.
599 Biol., **52**, 407-436, doi:10.1146/annurev.arplant.52.1.407, 2001.

600 Shepherd, T. G. and McLandress, C.: A Robust Mechanism for Strengthening of the Brewer–
601 Dobson Circulation in Response to Climate Change: Critical-Layer Control of Subtropical
602 Wave Breaking, J. Atmos. Sci., 68(4), 784–797, doi:10.1175/2010JAS3608.1, 2011.

603 Silva, R. A., West, J. J., Zhang, Y., Anenberg, S. C., Lamarque, J.-F., Shindell, D. T., Collins, W.
604 J., Dalsoren, S., Faluvegi, G., Folberth, G., Horowitz, L. W., Nagashima, T., Naik, V.,
605 Rumbold, S., Skeie, R., Sudo, K., Takemura, T., Bergmann, D., Cameron-Smith, P., Cionni,
606 I., Doherty, R. M., Eyring, V., Josse, B., MacKenzie, I. A., Plummer, D., Righi, M.,
607 Stevenson, D. S., Strode, S., Szopa, S. and Zeng, G.: Global premature mortality due to
608 anthropogenic outdoor air pollution and the contribution of past climate change, Environ. Res.
609 Lett., 8, 34005, doi:10.1088/1748-9326/8/3/034005, 2013.

610 Soden, B. and Held, I.: An Assessment of Climate Feedbacks in Coupled Ocean – Atmosphere
611 Models, J. Clim., 19(2003), 3354–3360, doi:10.1175/JCLI9028.1, 2006.

612 Solomon, S.: Stratospheric ozone depletion: A review of concepts and history, Rev. Geophys.,
613 37(3), 275–316, doi:10.1029/1999RG900008, 1999.

614 Stevenson, D. S. et al.: Multimodel ensemble simulations of present-day and near-future
615 tropospheric ozone, J. Geophys. Res., 111, D08301, doi:10.1029/2005JD006338, 2006.

© Author(s) 2017. CC-BY 3.0 License.

616 Stevenson, D. S., Young, P. J., Naik, V., Lamarque, J. F., Shindell, D. T., Voulgarakis, a., Skeie,
617 R. B., Dalsoren, S. B., Myhre, G., Berntsen, T. K., Folberth, G. a., Rumbold, S. T., Collins,
618 W. J., MacKenzie, I. a., Doherty, R. M., Zeng, G., Van Noije, T. P. C., Strunk, a., Bergmann,
619 D., Cameron-Smith, P., Plummer, D. a., Strode, S. a., Horowitz, L., Lee, Y. H., Szopa, S.,
620 Sudo, K., Nagashima, T., Josse, B., Cionni, I., Righi, M., Eyring, V., Conley, a., Bowman, K.
621 W., Wild, O. and Archibald, a.: Tropospheric ozone changes, radiative forcing and
622 attribution to emissions in the Atmospheric Chemistry and Climate Model Intercomparison
623 Project (ACCMIP), Atmos. Chem. Phys., 13(6), 3063–3085, doi:10.5194/acp-13-3063-2013,
624 2013.

625 Tang, Q., Hess, P. G., Brown-steiner, B. and Kinnison, D. E.: Tropospheric ozone decrease due
626 to the Mount Pinatubo eruption : Reduced stratospheric influx, Geophys. Res. Lett. , 40(July),
627 5553–5558, doi:10.1002/2013GL056563, 2013.

628 Tie, X., and Brasseur, G.: The response of stratospheric ozone to volcanic eruptions: Sensitivity
629 to atmospheric chlorine loading, Geophys. Res. Lett., 22, 3035-3038,
630 doi:10.1029/95GL03057.

631 Tilmes, S., Müller, R., and Salawitch, R.: The sensitivity of polar ozone depletion to proposed
632 geoengineering schemes, Science, 320, 1201-1204, doi:10.1126/science.1153966, 2008.

633 Tilmes, S., Garcia, R. R., Kinnison, D. E., Gettelman, A., and Rasch, P. J.: Impact of
634 geoengineered aerosols on the troposphere and stratosphere, J. Geophys. Res., 114, D12305,
635 doi:10.1029/2008JD011420, 2009.

636 Tilmes, S., Kinnison, D. E., Garcia, R. R., Salawitch, R., Canty, T., Lee-Taylor, J., Madronich,
637 S., and Chance, K.: Impact of very short-lived halogens on stratospheric ozone abundance
638 and UV radiation in a geo-engineered atmosphere, Atmos. Chem. Phys., 12, 10,945-10,955,
639 doi:10.5194/acp-12-10945-2012, 2012.

640 Tilmes, S. et al.: The hydrological impact of geoengineering in the Geoengineering Model
641 Intercomparison Project (GeoMIP), J. Geophys. Res. Atmos., 118, 11,036-11,058,
642 doi:10.1002/jgrd.50868, 2013.

643 Tilmes, S., Sanderson, B. M., and O'Neill, B. C.: Climate impacts of geoengineering in a
644 delayed mitigation scenario, Geophys. Res. Lett., 43, 8222-8229,
645 doi:10.1002/2016GL070122, 2016a.

646 Tilmes, S., Lamarque, J-F., Emmons, L. K., Kinnison, D. E., Marsh, D., Garcia, R. R., Smith, A.
647 K., Neely, R. R., Conley, A., Vitt, F., Val, M. M., Hiroshi, T., Simpson, I., Blake, D. R., and
648 Blake, N.: Representation of the Community Earth Sytem Model (CESM1) CAM4-chem
649 within the Chemistry-Climate Model Initiative (CCMI), Geoscientific Model Development, 9
650 (5), 1853-1890, doi:10.5194/gmd-9-1853-2016, 2016b.

651 Tilmes, S., et al.: A new Geoengineering Model Intercomparison Project (GeoMIP) experiment
652 designed for climate and chemistry models, Geosci. Model Dev., 8, 43-49, doi:10.5194/gmd-
653 8-43-2015, 2015.

654 Tingey, D. T., Manning, M., Grothaus, L. C., and Burns, W. F.: Influence of light and
655 temperature on monoterpene emission rates from Slash Pine. Plant Physiology, 65(5), 797-
656 801, doi: 10.1104/pp.65.5.797, 1980.

© Author(s) 2017. CC-BY 3.0 License.

657 Vingarzan, R.: A review of surface ozone background levels and trends, Atmos. Env., 38, 3431-
658 3442, doi:10.1016/j.atmosenv.2004.03.030, 2004.

659 Waugh, D.: Age of stratospheric air: Theory, observations, and models, Rev. Geophys., 40(4),
660 doi:10.1029/2000RG000101, 2002.

661 Wigley, T. M. L.: A combined mitigation/geoengineering approach to climate stabilization,
662 Science, 314, 452-454, doi:10.1126/science.1131728, 2006.

663 Wild, O.: Modelling the global tropospheric ozone budget: exploring the variability in current
664 models, Atmos. Chem. Phys., 7, 2643-2660, doi:10.5194/acp-7-2643-2007, 2007.

665 Wild, O. et al.: Modelling future changes in surface ozone: a parameterized approach, Atmos.
666 Chem. Phys., 12, 2037-2054, doi:10.5194/acp-12-2037-2012, 2012.

667 Wilton, D. J., Hewitt, C. N., and Beerling, D. J.: Simulating effect of changes in direct and
668 diffuse radiation on canopy scale isoprene emissions from vegetation following volcanic
669 eruptions, Atmos. Chem. Phys., 11, 11723-11731, doi:10.5194/acp-11-11723-2011, 2011.

670 Xia, L., Robock, A., Tilmes, S., and Neely III, R. R.: Stratospheric sulfate geoengineering could
671 enhance the terrestrial photosynthesis rate, Atmos. Chem. Phys., 16, 1479-1489,
672 doi:10.5194/acp-16-1479-2016, 2016.

673 Young, P. J. et al.: Pre-industrial to end 21st century projections of tropospheric ozone from the
674 Atmospheric Chemistry and Climate Model Intercomparison Project (ACCMIP), Atmos.
675 Chem. Phys., 13, 2063-2090, doi:10.5194/acp-13-2063-2013, 2013.

676

Atmos. Chem. Phys. Discuss., doi:10.5194/acp-2017-434, 2017
Manuscript under review for journal Atmos. Chem. Phys.
Discussion started: 19 May 2017
© Author(s) 2017. CC-BY 3.0 License.

Atmospheric Chemistry and Physics Discussions

677 **Table 1.** Tropospheric ozone production and loss rates (Tg yr^{-1}) over the period of years 2030-
678 2069 (average of three ensemble members). For chemical ozone production and ozone loss the
679 net impacts of only the most important reaction pathways are listed.

	RCP6.0	G4SSA	G4SSA-S
O_3 Net Chemical Change	346.1	472.7	384.8
O_3 Tropospheric Dry Deposition	901.5	891.5	909.4
O_3 STE*	555.4	418.8	524.6
O_3 Production	4895.8	4764.0	4671.8
r-NO-HO_2	3087.3	3031.0	2964.8
r-CH_3O_2-NO	1132.3	1105.2	1083.1
r-PO_2-NO	21.8	20.1	19.9
r-CH_3CO_3-NO	183.1	172.2	171.2
r-C_2H_5O2-NO	6.6	6.7	6.7
0.92*r-$ISOPO_2$-NO	149.8	135.3	134.0
r-$MACRO_2$-NOa	76.1	69.8	69.5
r-MCO_3-NO	34.5	30.5	30.3
r-RO_2-NO	12.2	11.5	11.5
r-XO_2-NO	66.5	60.8	60.5
0.9*r-$TOLO_2$-NO	4.1	4.1	4.1
r-$TERPO_2$-NO	18.1	16.9	16.8
0.9*r-$ALKO_2$-NO	22.9	23.0	22.9
r-$ENEO_2$-NO	12.5	11.6	11.7
r-EO_2-NO	36.8	34.6	34.5
r-$MEKO_2$-NO	17.7	17.9	17.8
0.4*r-ONITR-OH	7.5	6.8	6.8
r-jonitr	1.4	1.2	1.2
O_3 Loss	4421.1	4158.6	4151.6
r-O(1D)-H_2O	2430.4	2286.5	2263.5
r-OH-O_3	548.2	528.3	527.0
r-HO_2-O_3	1288.9	1216.7	1232.9
r-C_3H_6-O_3	13.8	11.5	11.5
0.9*r-ISOP-O_3	71.4	58.0	57.6
r-C_2H_4-O_3	9.3	7.8	8.0
0.8*r-MVK-O_3	18.6	15.5	15.7
0.8*r-MACR-O_3	3.5	2.9	2.9
r-$C_{10}H_{16}$-O_3	37.0	31.5	31.6

680 *O_3 STE is ozone transported through the Stratosphere Troposphere Exchange. We calculated
681 this value using equation –

682 $$O_{3\ STE} + O_{3\ net\ tropospheric\ chemical\ change} + O_{3\ dry\ tropospheric\ deposition} = 0$$

683 Tropospheric ozone is defined as ozone concentration less than 150 ppb.

Atmos. Chem. Phys. Discuss., doi:10.5194/acp-2017-434, 2017
Manuscript under review for journal Atmos. Chem. Phys.
Discussion started: 19 May 2017
© Author(s) 2017. CC-BY 3.0 License.

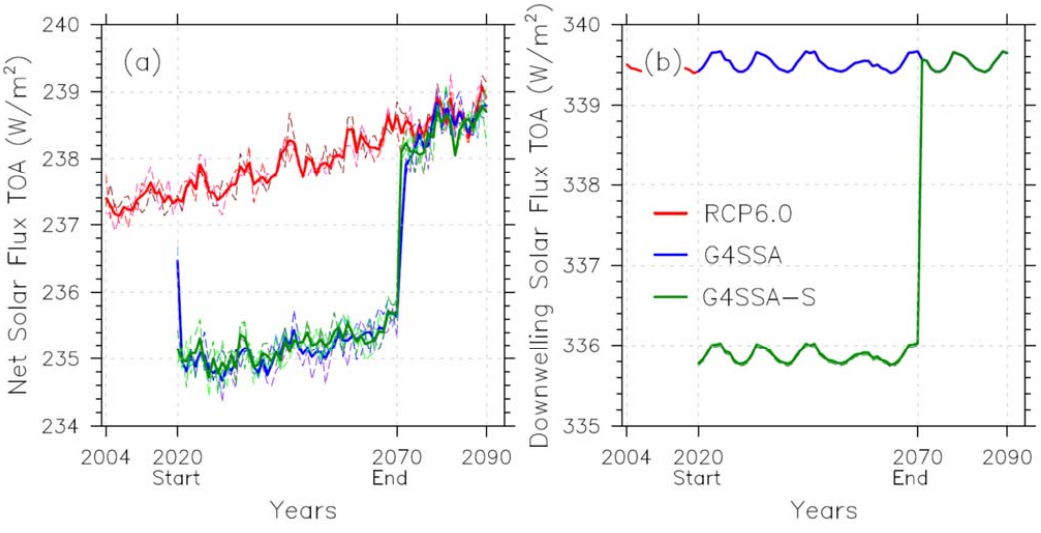

Figure 1. (a) Global averaged annual net solar flux on the top of the atmosphere (W/m^2) and (b) downwelling solar flux on the top of the atmosphere (W/m^2). Dashed lines are ensemble members, and solid lines are the average of three ensemble members. Geoengineering starts at January 1st 2020 and ends at January 1st 2070. The 11-year periodicity is imposed as a prediction of the sunspot cycle. In (b) the G4SSA curve exactly covers the RCP6.0 curve.

Atmos. Chem. Phys. Discuss., doi:10.5194/acp-2017-434, 2017
Manuscript under review for journal Atmos. Chem. Phys.
Discussion started: 19 May 2017
© Author(s) 2017. CC-BY 3.0 License.

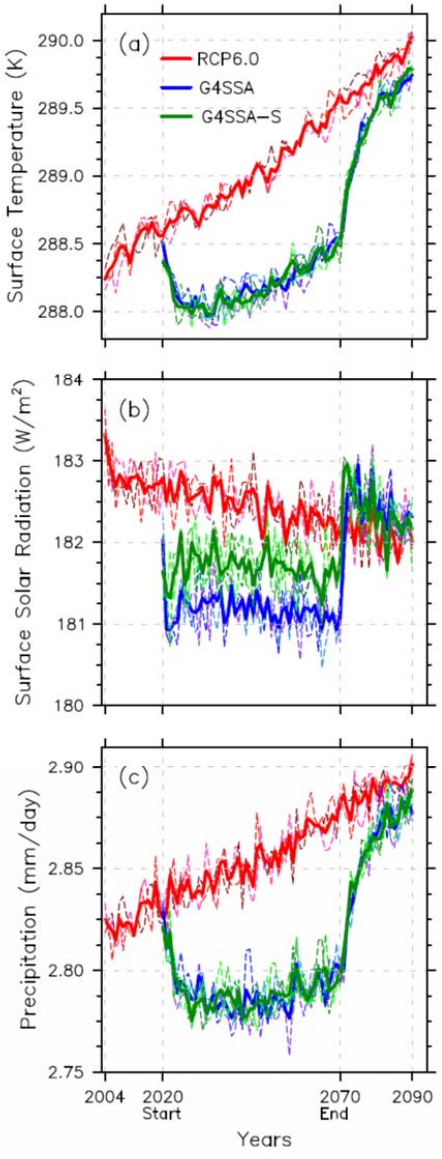

Figure 2. (a) Global averaged annual surface air temperature (K), (b) downwelling surface solar radiation (W/m^2), and (c) Land average annual canopy transpiration (mm/day). Dashed lines are ensemble members, and solid lines are the average of the three ensemble members. Geoengineering starts at 1 January 2020 and ends at 1 January 2070.

Atmos. Chem. Phys. Discuss., doi:10.5194/acp-2017-434, 2017
Manuscript under review for journal Atmos. Chem. Phys.
Discussion started: 19 May 2017
© Author(s) 2017. CC-BY 3.0 License.

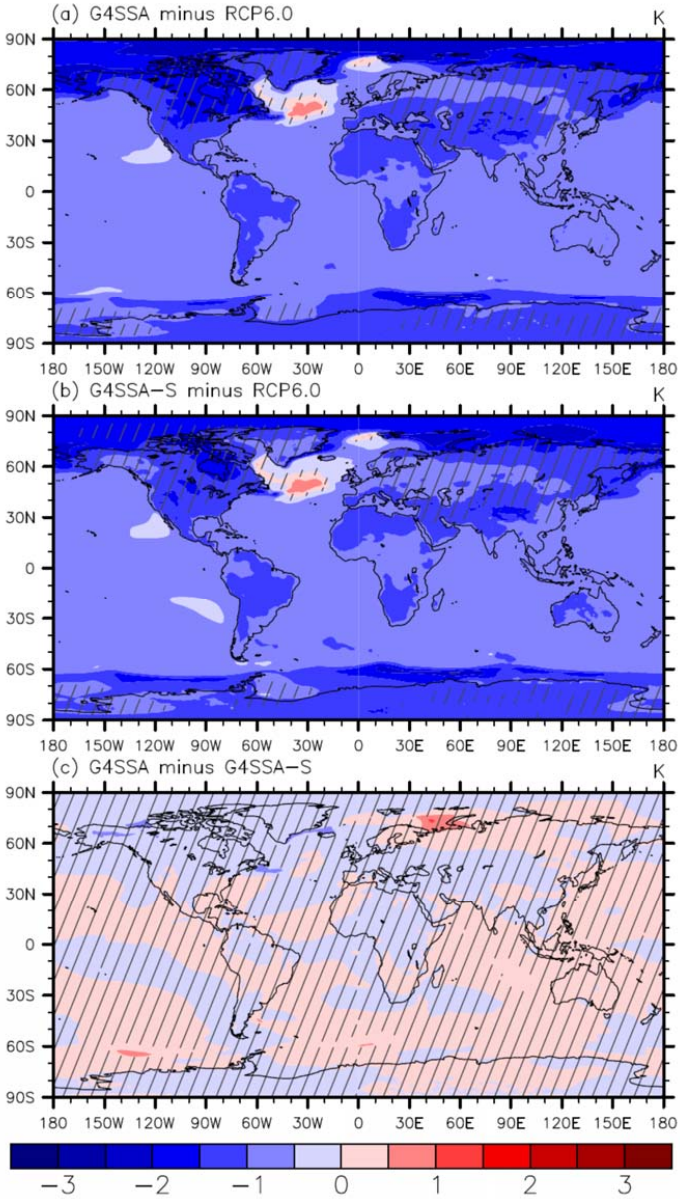

Figure 3. Global maps of surface temperature differences (K) between (a) G4SSA and RCP6.0, (b) G4SSA-S and RCP6.0, and (c) G4SSA and G4SSA-S over the period 2030-2069. Hatched regions are areas with $p > 0.05$ (where changes are not statistically significant based on a paired *t*-test).

Atmos. Chem. Phys. Discuss., doi:10.5194/acp-2017-434, 2017
Manuscript under review for journal Atmos. Chem. Phys.
Discussion started: 19 May 2017
© Author(s) 2017. CC-BY 3.0 License.

Atmospheric Chemistry and Physics Discussions

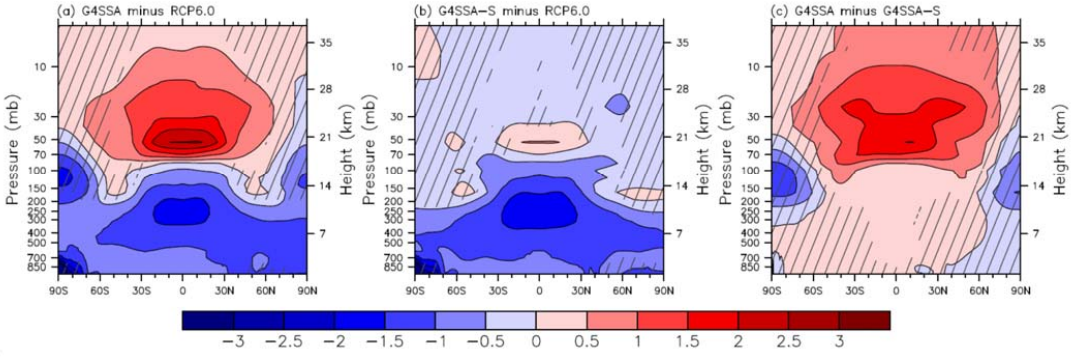

Figure 4. Zonal mean temperature differences (K) in the geoengineering experiments (a) G4SSA minus RCP6.0, (b) G4SSA-S minus RCP6.0, and (c) G4SSA minus G4SSA-S. These are averaged for three ensemble members for years 2030-2069. Hatched regions are insignificant, with $p > 0.05$.

Atmos. Chem. Phys. Discuss., doi:10.5194/acp-2017-434, 2017
Manuscript under review for journal Atmos. Chem. Phys.
Discussion started: 19 May 2017
© Author(s) 2017. CC-BY 3.0 License.

Atmospheric Chemistry and Physics Discussions

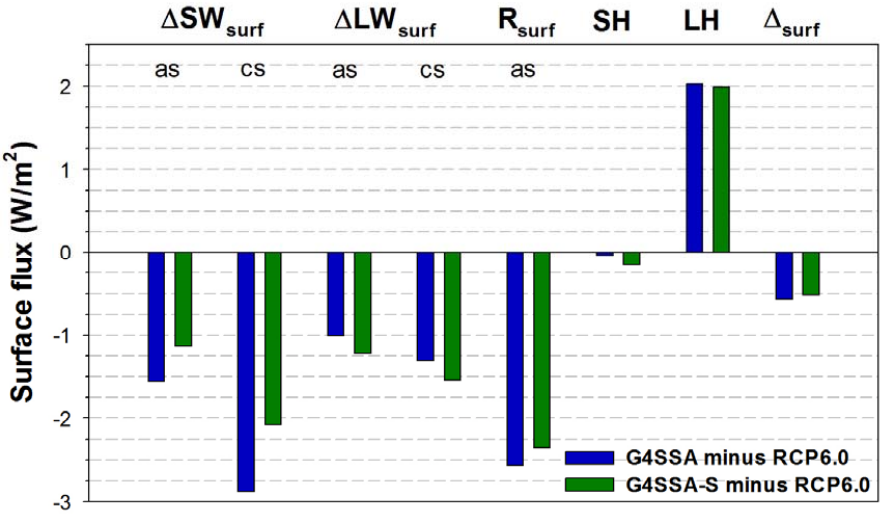

708
709 **Figure 5**. Energy flux at the surface, shown as G4SSA minus RCP6.0 and G4SSA-S minus
710 RCP6.0 for 2030-2069. For all fluxes, downwelling is positive. ΔSW_{surf} is the net shortwave
711 flux at the surface, ΔLW_{surf} is the net longwave flux at the surface, R_{surf} is the sum of ΔSW_{surf} and
712 ΔLW_{surf}, SH is sensible heat, LH is latent heat, and ΔL is the sum of ΔSW_{surf}, ΔLW_{surf}, SH, and
713 LH; as is all sky and cs is clear sky.
714
715

Atmos. Chem. Phys. Discuss., doi:10.5194/acp-2017-434, 2017
Manuscript under review for journal Atmos. Chem. Phys.
Discussion started: 19 May 2017
© Author(s) 2017. CC-BY 3.0 License.

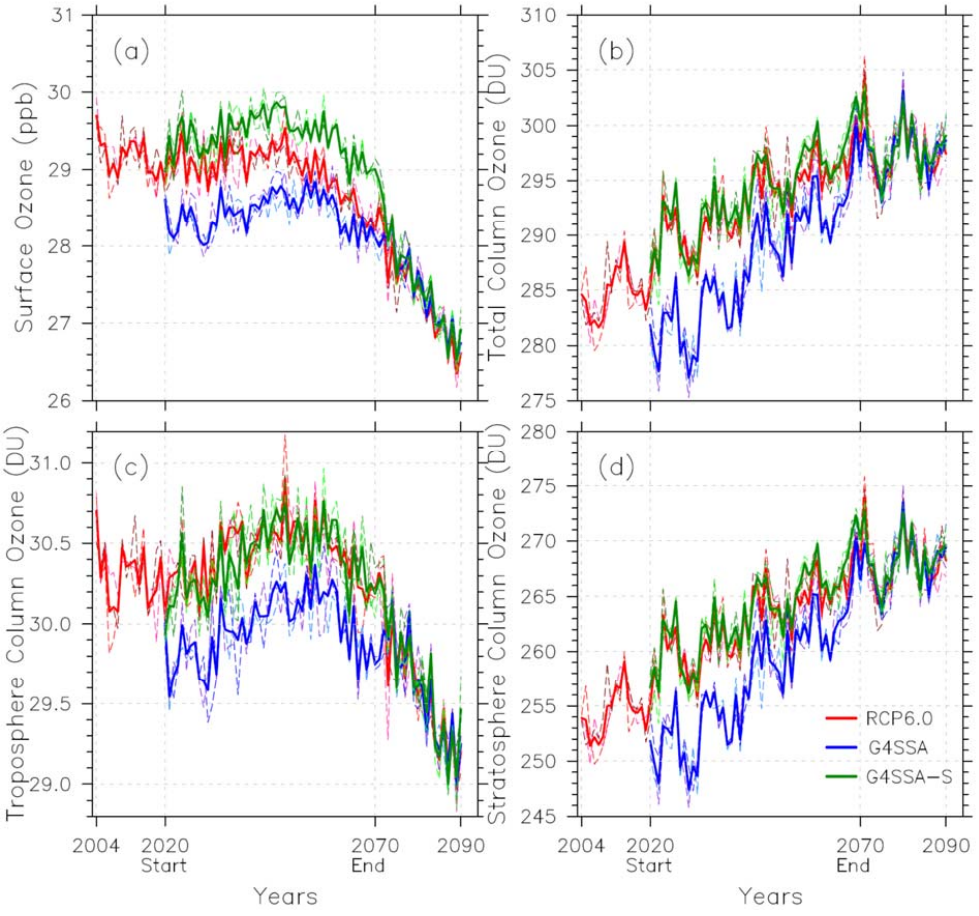

716

717 **Figure 6.** (a) Global averaged annual surface ozone concentrations (ppb), (b) total column
718 ozone (DU), (c) tropospheric column ozone (DU), and (d) stratospheric column ozone (DU).
719 Ozone concentration of 150 ppb is used as the boundary of tropospheric ozone and stratospheric
720 ozone. Dashed lines are ensemble members, and solid lines are the average of the three
721 ensemble members. Geoengineering starts at 1 January 2020 and ends at 1 January 2070.
722
723

Atmos. Chem. Phys. Discuss., doi:10.5194/acp-2017-434, 2017
Manuscript under review for journal Atmos. Chem. Phys.
Discussion started: 19 May 2017
© Author(s) 2017. CC-BY 3.0 License.

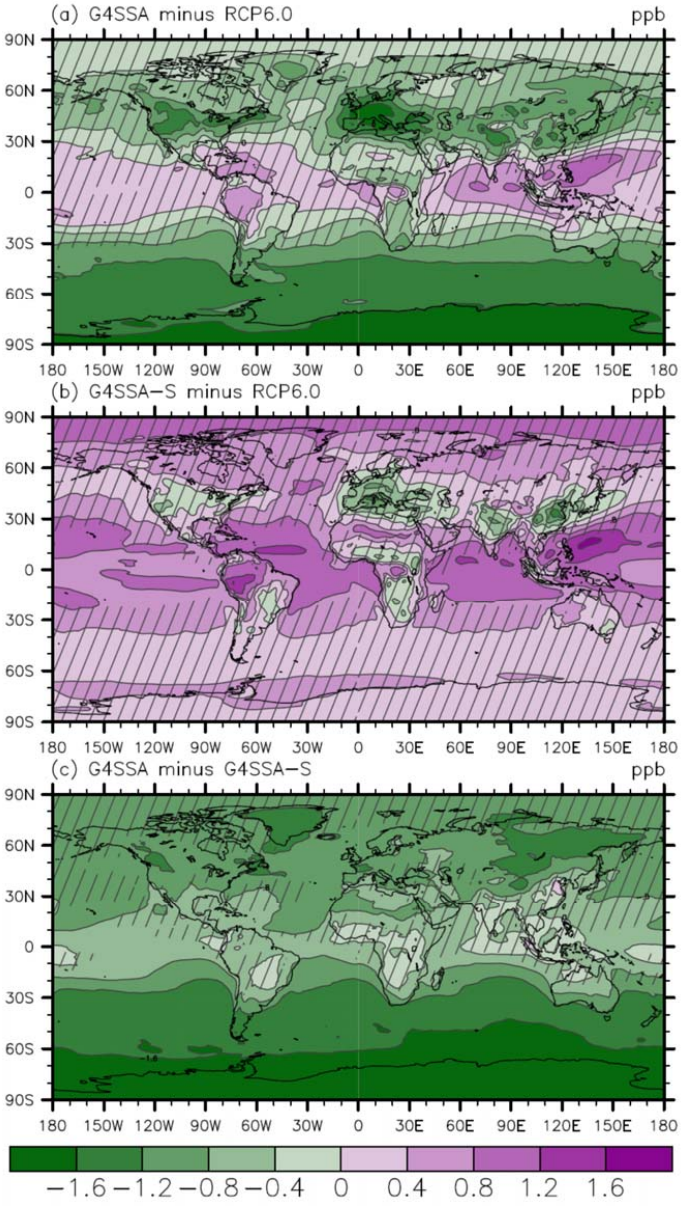

724

725 **Figure 7**. Global maps of surface ozone concentration differences (ppb) between (a) G4SSA
726 and RCP6.0, (b) G4SSA-S and RCP6.0, and (c) G4SSA and G4SSA-S for 2030-2069. Hatched
727 regions are insignificant, with $p > 0.05$.
728

Atmos. Chem. Phys. Discuss., doi:10.5194/acp-2017-434, 2017
Manuscript under review for journal Atmos. Chem. Phys.
Discussion started: 19 May 2017
© Author(s) 2017. CC-BY 3.0 License.

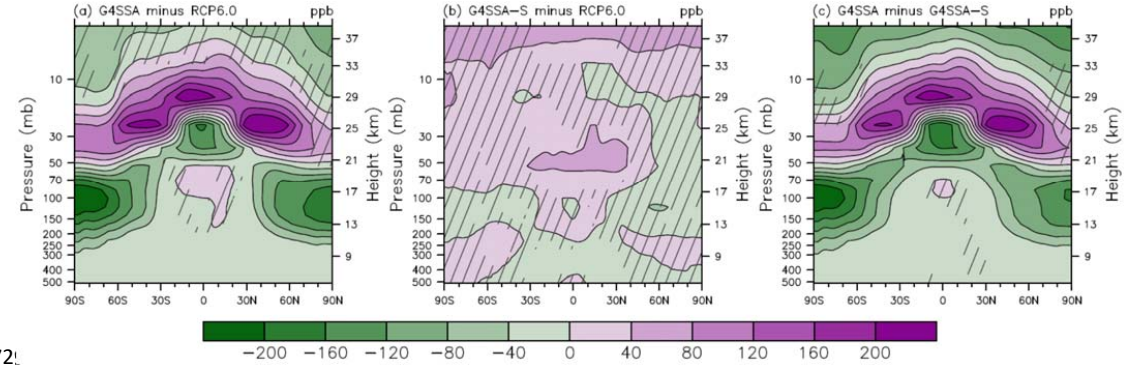

Figure 8. Zonal mean ozone concentration differences (ppb) in the geoengineering experiments, averaged for three ensemble members for 2030-2069. Hatched regions are insignificant, with $p >$ 0.05.

Atmos. Chem. Phys. Discuss., doi:10.5194/acp-2017-434, 2017
Manuscript under review for journal Atmos. Chem. Phys.
Discussion started: 19 May 2017
© Author(s) 2017. CC-BY 3.0 License.

Atmospheric Chemistry and Physics Discussions

734

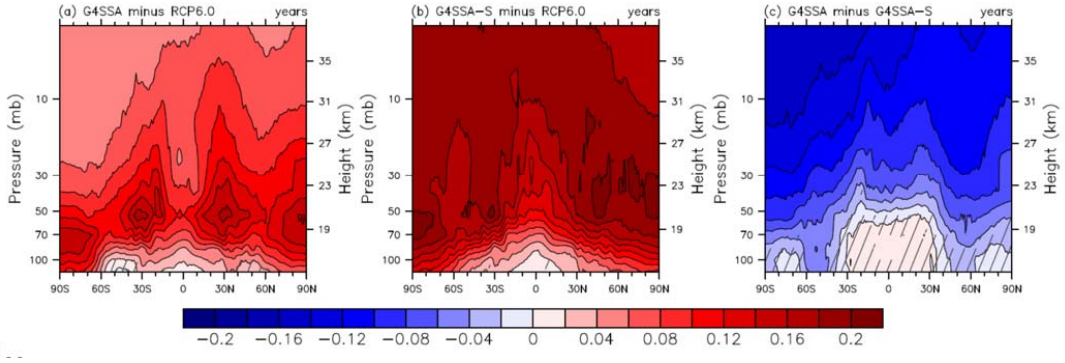

736 **Figure 9.** Zonal mean age of air differences (years) between (a) G4SSA and RCP6.0, (b)
737 G4SSA-S and RCP6.0, and (c) G4SSA and G4SSA-S. They are averaged for three ensemble
738 members for 2030-2069. Hatched regions are insignificant, with $p > 0.05$.

739

Atmos. Chem. Phys. Discuss., doi:10.5194/acp-2017-434, 2017
Manuscript under review for journal Atmos. Chem. Phys.
Discussion started: 19 May 2017
© Author(s) 2017. CC-BY 3.0 License.

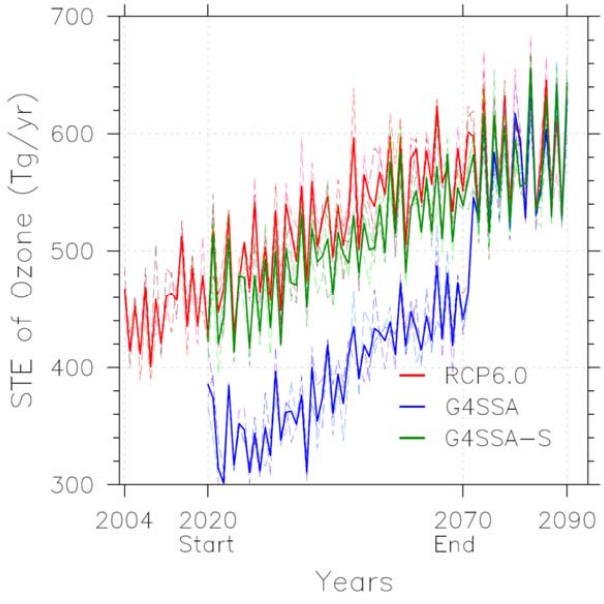

740

741 **Figure 10.** Global annual averaged ozone transported from the stratosphere to the troposphere
742 (STE of ozone) in Tg yr^{-1}. Geoengineering starts at 1 January 2020 and ends at 1 January 2070.